ELSEVIER

SHORT COMMUNICATION

Effect of 2, 5, 7, and 9at.% Al on the Solution Heat-Treated (1280°C, 50 hours, Water Quenched) Structure of Ni-20at.% Mo Alloy

Elaine Shen,* Charlie R. Brooks,* and E. A. Kenik†

**Materials Science and Engineering Department, The University of Tennessee, Knoxville, Tennessee 37996, USA; and †Metals and Ceramics Division, Oak Ridge National Laboratory, Oak Ridge, Tennessee 37831, USA*

INTRODUCTION

The alloy Ni-20at.% Mo is a face-centered cubic (fcc) solid solution (α) above 868°C, and at equilibrium has a long-range ordered (LRO) structure (designated β) below this temperature [1]. The α structure can be retained by sufficiently rapid cooling (e.g., water quenching). However, the structure is not a random solid solution, but exhibits short-range order (SRO). Its presence can be easily detected in the (001) electron diffraction pattern by the appearance of diffuse maxima at {1,1/2,0} positions, as shown in Fig. 1a. (All diffraction indices are referred to the parent fcc lattice.) If the structure is LRO β, the pattern shows superlattice spots, as shown in Fig. 1b. If the α has begun to decompose to β, the pattern appears as shown in Fig. 1c [2]. The SRO structure appears to be a characteristic of the high temperature α phase. For example, Cao et al. [2] observed the diffuse SRO spots in splat-cooled samples where the cooling rate was approximately 10^6K/sec.

In this study, we have determined the effect of 2, 5, 7, and 9at.% Al additions to the base Ni-20at.% Mo alloy on the as-quenched hardness and structure. Samples were quenched from 1280°C, and the Ni-Mo-Al phase diagram [3] in Fig. 2 indicates that all alloys should be in the α region at 1250°C.

EXPERIMENTAL PROCEDURE

The alloys were prepared by arc-melting pieces of a Ni-20at.% Mo base alloy of the composition in Table 1 with pieces of high purity aluminum (99.99wt.% Al). The compositions of the alloys are listed in Table 2, and are based on the weighed amounts of the starting material, and not chemical analyses. Note that for all alloys the Ni-Mo ratio is about 4.0. Melting was carried out in a conventional, cold hearth, arc-casting furnace using a nonconsumable tungsten electrode and a low partial pressure of argon. The samples were turned 4–5 times and remelted to ensure homogeneity. Samples were encapsulated in silica tubes, which were evacuated and then backfilled with high purity argon at a reduced pressure. One set of samples in silica tubes was heated to 1250°C (±10°C) for 50 hours, followed by breaking the tubes under water at 25°C (water quenching). Optical microscopy showed that in this condition all the alloys were single phase except for the 9at.% alloy. A second set of samples, encapsulated in silica tubes as the other set, was heated to 1280°C for 50 hours, then quenched as before. However, this set did not include the 9at.% Al alloy due to limited material. Note that the 9at.% Al alloy was solution heat treated for 50 hours at 1250°C, whereas all the other alloys were heat treated for 50 hours

MATERIALS CHARACTERIZATION 43:57–68 (1999)
© Elsevier Science Inc., 1999. All rights reserved.
655 Avenue of the Americas, New York, NY 10010

1044-5803/99/$–see front matter
PII S1044-5803(99)00005-4

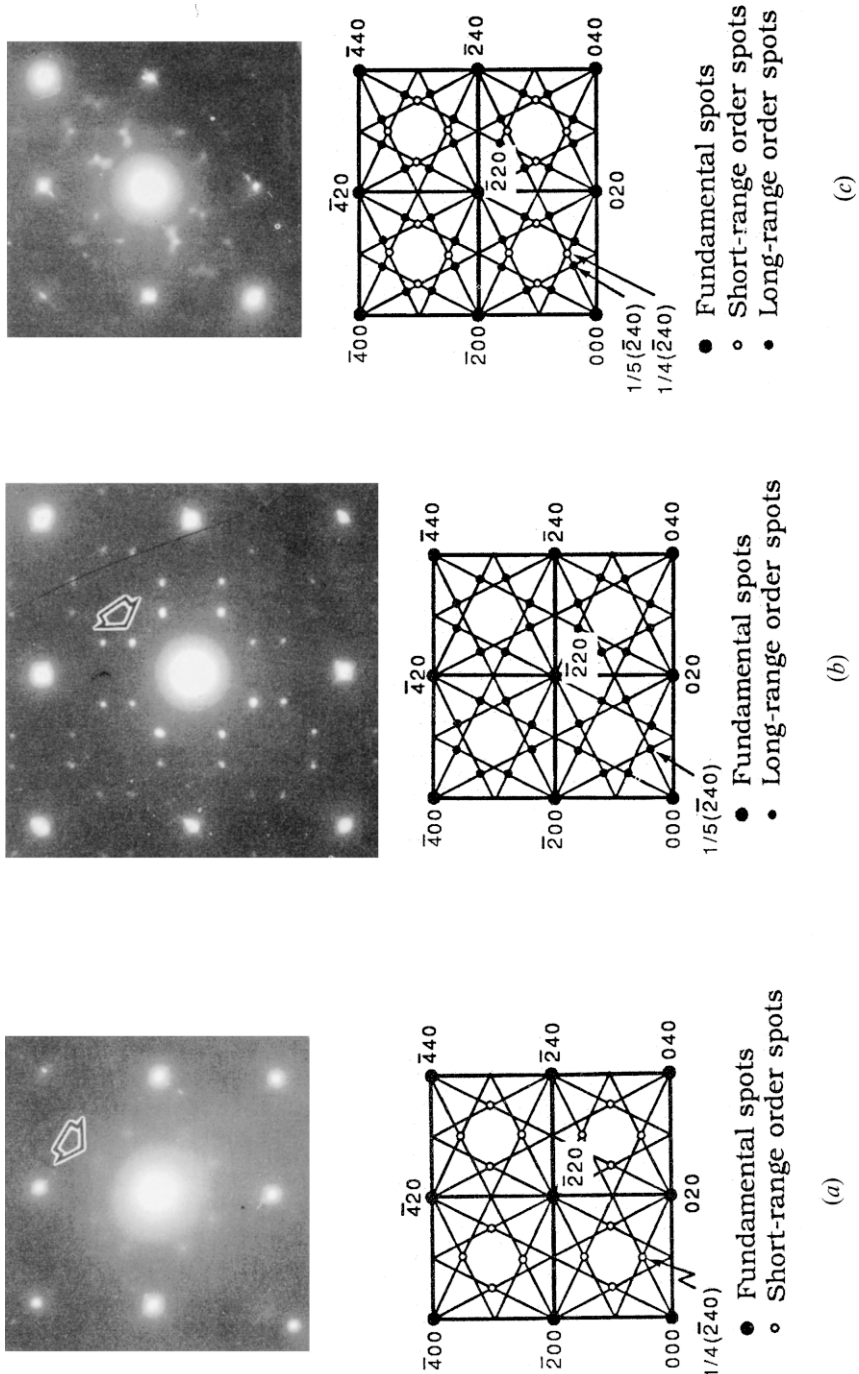

FIG. 1. (1001) Electron diffraction patterns for a Ni-20at.% Mo alloy. (a) SRO α, showing diffuse spots (arrow); (b) long-range ordered β, showing LRO spots (arrow); (c) pattern showing the transition from α to β. Source: [2].

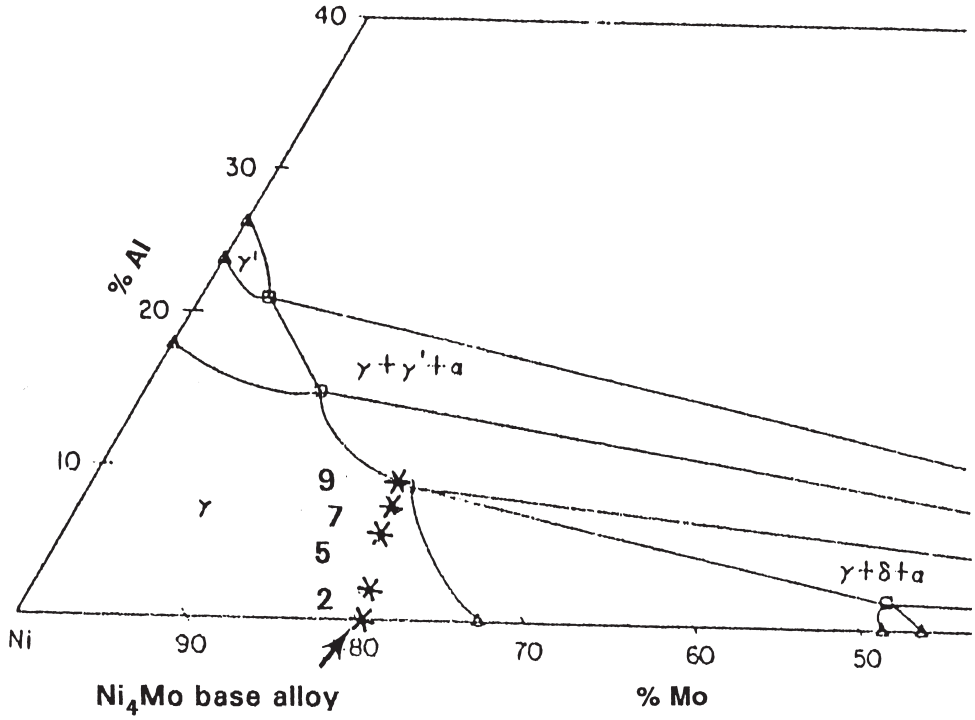

FIG. 2. The Ni-Mo-Al phase diagram at 1260°C [3]. The composition of the alloys of this study are noted by the crosses.

at 1250°C, then reheat treated for 50 hours at 1280°C.

For transmission electron microscopy (TEM) examination, slices ~1-mm thick were cut from each solution heat treated ingot using a thin, high-speed, abrasive, cut-off wheel with copious water for cooling. From these slices 3-mm discs were punched. Each disk was then further reduced to about 0.3mm thickness by slow hand grinding on wet 600 grade SiC paper. The center of the disks was thinned to electron transparency by a twin jet polishing apparatus with a light detection system to minimize over-etching. The samples were thinned electrolytically first in a solution of 640ml H_3PO_4, 150ml H_2SO_4, 35ml HCl, and 210ml water, followed in some cases by further thinning in a solution of 175ml butanol, 30ml HCl, and 300ml methanol. For the former electrolyte, the operating conditions were 5–10V, 0.3–0.5A, and −25–10°C. For the latter solution, they were 30–40V, 0.3–0.5A, and −5–0°C. After thinning, the samples were rinsed in distilled water, then methanol, and air-dried on lint-free paper. To enhance the electron transparency, this thinning usually was followed by ion mill-

Table 1 Chemical Analysis of the Base Alloy Used to Make the Ternary Alloys

Element	*at.%*	*wt.%*
Ni	80.0	70.5
Mo	20.0	29.5
Al	<0.0003	<0.01
O	0.0001	0.003

Table 2 Nominal Chemical Composition of the Alloys Studied

Ni		*Mo*		*Al*		*Ni/Mo*
at.%	*wt.%*	*at.%*	*wt.%*	*at.%*	*wt.%*	*ratio*
78	69.8	20	29.2	2	1.0	3:9
76	69.1	19	28.9	5	2.0	4:0
74	68.4	19	28.6	7	3.0	3:9
73	67.7	18	28.3	9	4.0	4:1

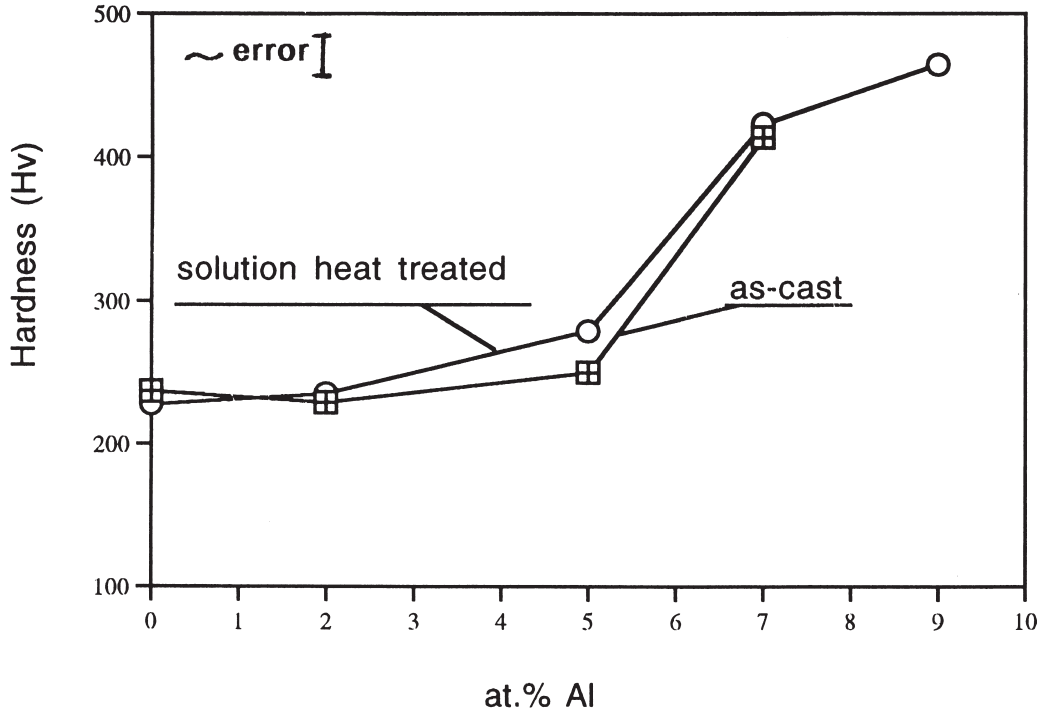

FIG. 3. Hardness as a function of Al content for the solution heat-treated condition (1250°C, 50 hours, water quenched, then 1280°C, 50 hours, water quenched, except for the 9at.% Al alloy which was 1250°C, 50 hours). Also shown are data for the as-cast condition.

ing. The operating parameters were 6V, 12–15° tilt, 0.5–0.6A gun current, a milling time of 30 min, and thinning was at −196°C to minimize preparation artifacts. The samples were examined in a Philips CM-12 transmission electron microscope operated at 120kV.

Microhardness measurements were made on metallographically polished, etched samples with a load of 500g. At least three measurements were made on each sample, and the average value is reported. The accuracy is approximately ±10 DPH.

RESULTS

HARDNESS

The effect of Al on the hardness of the solution heat treated alloys is shown in Fig. 3. Data are also shown for the as-cast condition. The hardness increases gradually up to 5at.% Al, but markedly increases to about 470DPH at 9at.% Al. The as-cast hardness is about the same as that of the solution heat treated condition.

OPTICAL MICROSCOPY

After the first solution heat treatment, examination of the microstructure using both light and scanning electron microscopy revealed what appeared to be a single phase structure for the 0, 2, 5, and 7at.% Al alloys (Figs. 4a–d). This observation is consistent with the phase diagram at 1260°C in Fig. 2, since the compositions of the alloys lie within the single phase α region. The TEM examination was of samples which had the additional solution heat treatment, and they were single phase. It is assumed that the second solution heat treatment produced a single phase microstructure for these alloys as shown in Figs. 4a–d. The 9at.% Al alloy showed second phase particles (arrows, Fig. 4e); according to Fig. 2, this could be a small amount of the α

phase. However, TEM examination did not detect any second phase.

TRANSMISSION ELECTRON MICROSCOPY

Characterization of the structure of Ni-rich Ni-Mo alloys is especially convenient by examination of the (001) electron diffraction pattern. (112) patterns are also useful. The well-known [1] diffuse spots of the short-range ordered α phase are shown in Fig. 1a for a binary Ni-20at.% Mo alloy. The (001) pattern from three variants of the long-range ordered β is shown in Fig. 1b; the superlattice spots are at distinctly different locations from the SRO spots.

Figure 5b shows a (001) pattern for the present water-quenched Ni-20at.% Mo base alloy. A SRO diffuse spot is indicated by the arrow. The microstructure from which the pattern was obtained is shown in

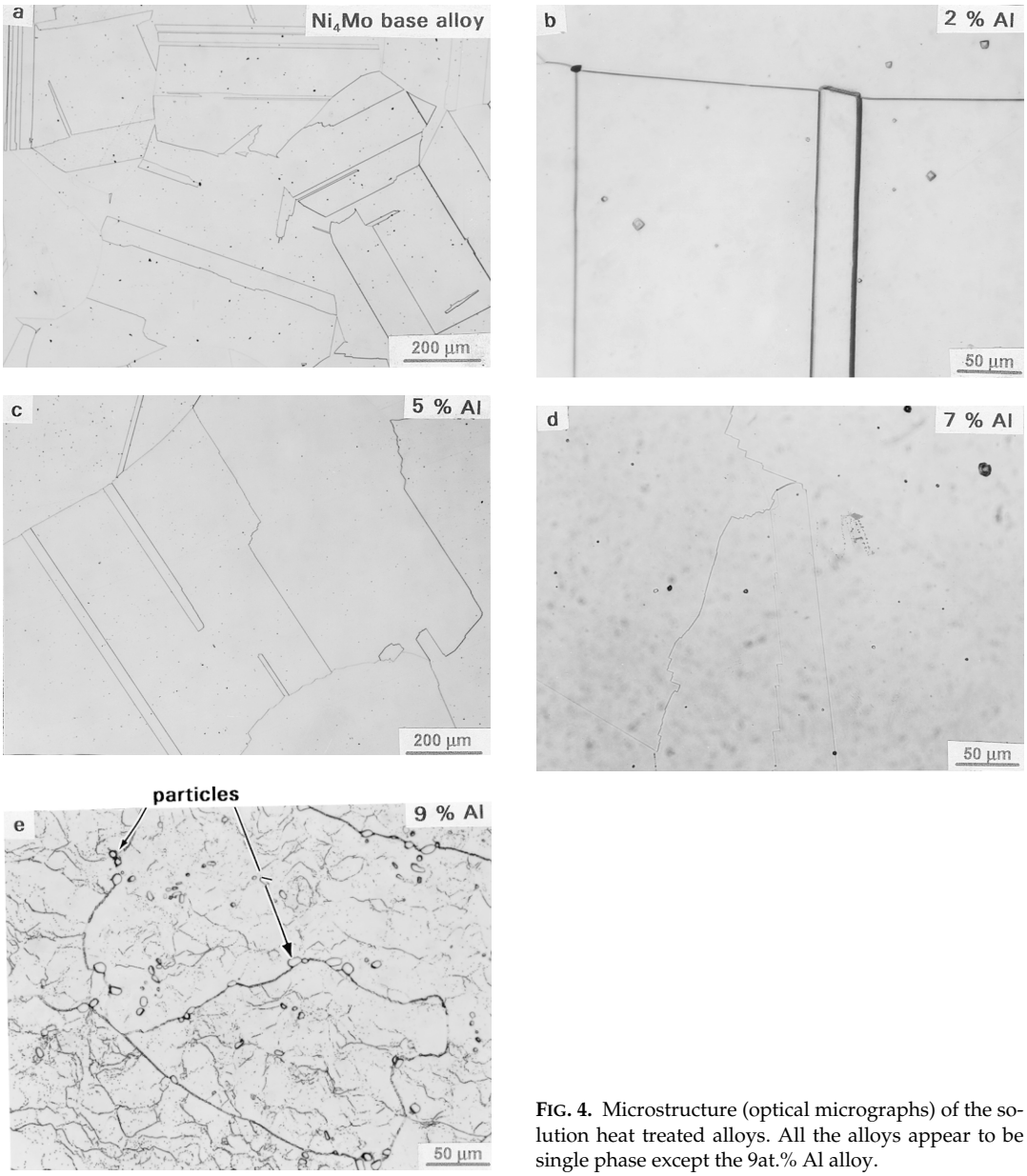

FIG. 4. Microstructure (optical micrographs) of the solution heat treated alloys. All the alloys appear to be single phase except the 9at.% Al alloy.

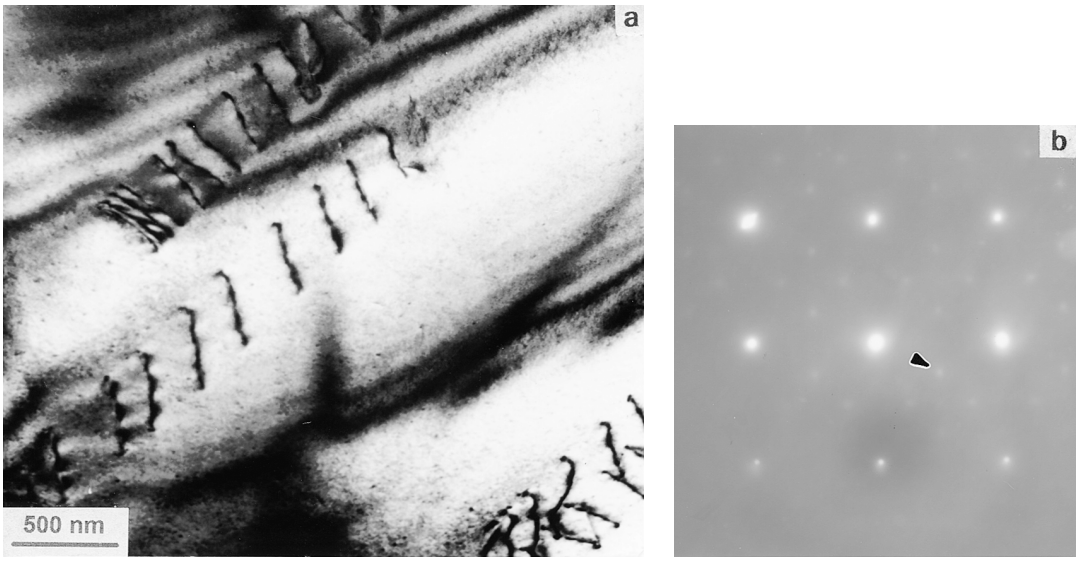

FIG. 5. Microstructure and (001) diffraction pattern of solution heat treated Ni-20at.% Mo base alloy. Only SRO α is present. A SRO diffraction spot is noted by the arrow, but these spots are very weak.

Fig. 5a. There are dislocation arrays present and the structure has a fine mottled appearance.

In the Al-containing alloys, other phases in addition to SRO α appeared. These were identified by comparison with the known (001) and (112) patterns shown in Fig. 6 [4, 5, 6] for the equilibrium phases β (Ni_4Mo), γ (Ni_3Mo), and γ′ ($Ni_3(Al,Mo)$), and the nonequilibrium phases DO_{22} (Ni_3Mo) and (Ni_2Mo).

The microstructure of the 2at.% Al alloy showed a fine mottled appearance (Fig. 7a). The diffraction pattern consisted of (Fig. 7b) SRO α diffuse spots (at "a") and DO_{22} spots (at "b") (compare with Fig. 6). The 5at.% Al alloy showed a similar structure (Fig. 8a), but the (112) pattern (Fig. 8b) did not contain any diffuse SRO α spots. The spots could all be identified with the DO_{22} structure.

The structure of the 7at.% Al alloy, which is also mottled, is shown in Fig. 9a. Comparison of the diffraction pattern (Fig. 9b) with those in Fig. 6 shows that the structure consists of the two phases DO_{22} and Ni_2Mo. The same two phases were found in the 9at.% Al alloy (Fig. 10), which also had a fine mottled structure.

DISCUSSION

The arrangement of the Ni and Mo atoms in SRO α in the Ni-20at.% Mo alloy has been the subject of extensive scrutiny. The status was reviewed by Brooks et al. [1] in 1984. At that time there were two models. One considered the SRO α to consist of fine microdomains of β [7, 8], and the other considered the structure to consist of concentration wave packets [9–13]. Since then, subsequent microstructural observations [14, 15] have not clarified this situation. It has not been possible to attain quenched α without SRO being present, even upon splat cooling [2]. The SRO can be destroyed by electron irradiation of either the SRO α or of LRO β, and low temperature annealing will restore them [16–18].

In the binary Ni-Mo alloys, it is clear that the α phase has a SRO structure at high temperature. It is well documented that upon aging the α phase below the order-disorder temperature of 868°C [1], in the lower temperature range (e.g., 600°C) the formation of the ordered β is preceded by the formation of the non-equilibrium DO_{22} [19–22] or the non-equilibrium Ni_2Mo phases [21–23]. In the Ni-Mo-Al alloys, the

appearance of these phases in the solution-treated condition raises the question whether they are present at the solution-treatment temperature and are retained upon quenching. However, the phase diagram indicates that only α is present. An alternative explanation is that these phases formed during cooling, and that the Al enhances the kinetics of the formation of these phases on cooling so that their formation

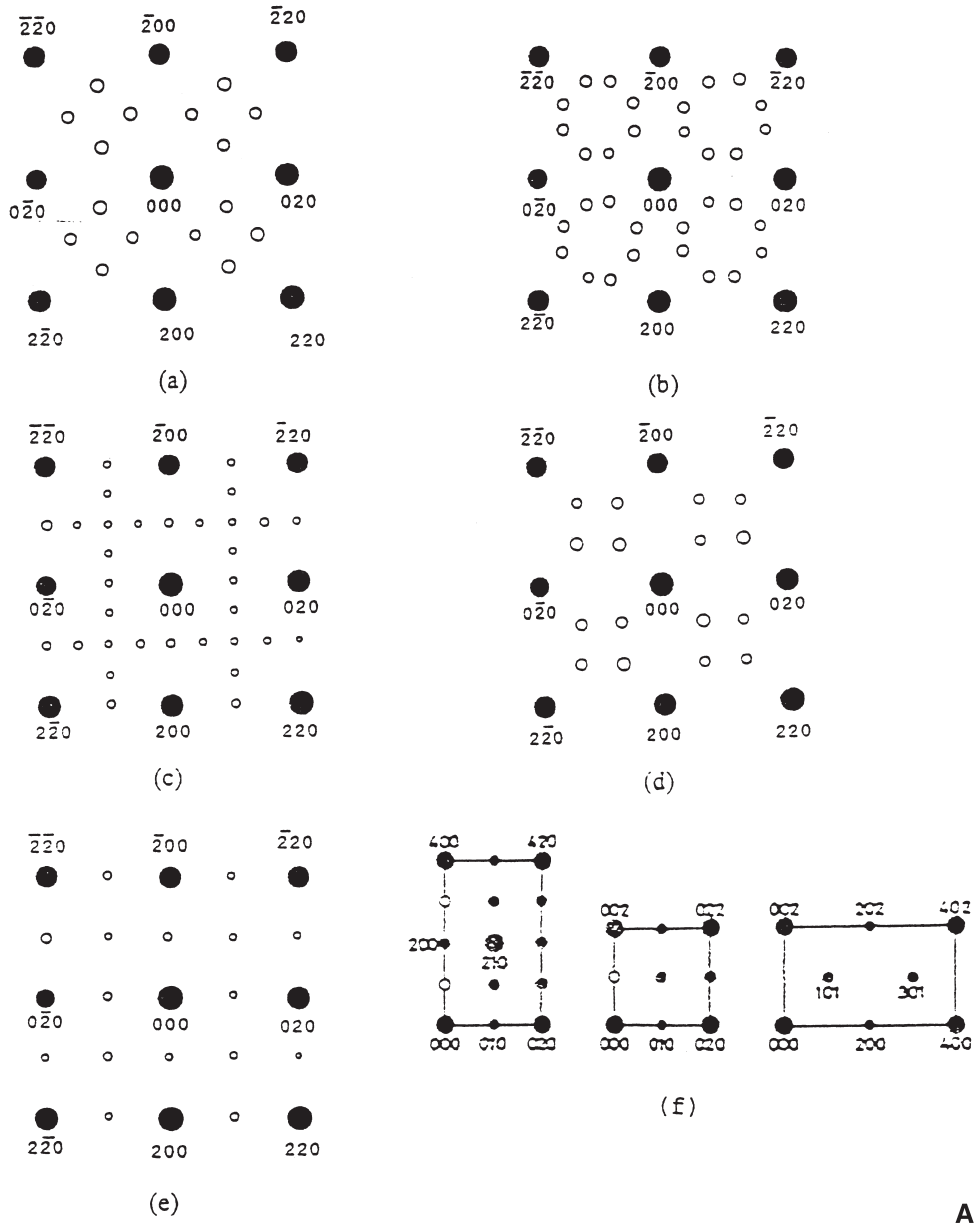

FIG. 6. Predicted (composite A: panels a–f) (001) and (composite B: panels a–e) (112) electron diffraction patterns for several phases which appear in Ni-Mo-Al alloys (adapted from [4, 5, 6]). (A) ● fundamental spots, ○ superlattice spots, (a) SRO α phase equilibrium, (b) β phase (Ni_4Mo) equilibrium, (c) DO_{22} (Ni_3Mo) non-equilibrium, (d) Pt_2Mo (Ni_2Mo) non-equilibrium, (e) LRO γ′ (Ni_3Al) equilibrium, (f) LRO γ (Ni_3Mo) equilibrium; (B) ● fundamental spots, ○ superlattice spots, (a) SRO α phase equilibrium, (b) β phase (Ni_4Mo) equilibrium, (c) DO_{22} (Ni_3Mo) non-equilibrium, (d) Pt_2Mo (Ni_2Mo) non-equilibrium, (e) LRO γ′ (Ni_3Al) equilibrium.

was not prevented at the cooling rate associated with breaking the silica tubes under water. To evaluate this effect, a sample of the 2at.% Al alloy was heated unprotected (no silica tube) in air for 20 min. at 1250°C, then quenched into water. Electron diffraction patterns showed only SRO α present, and no DO_{22} structure present. This is taken as evidence that the cooling rate upon breaking the silica tubes was not sufficiently high to prevent the formation of the metastable phase on cooling. It is concluded that increasing Al content enhanced the kinetics of the formation of the DO_{22} and Ni_2Mo phases during cooling.

For a Ni-14 at.% Mo-7at.% Al alloy, Agaronik et al. [24] have reported a somewhat different result. They water quenched thin strips (e.g., 10μm) of the alloy from 1200°C and found the structure contained SRO α

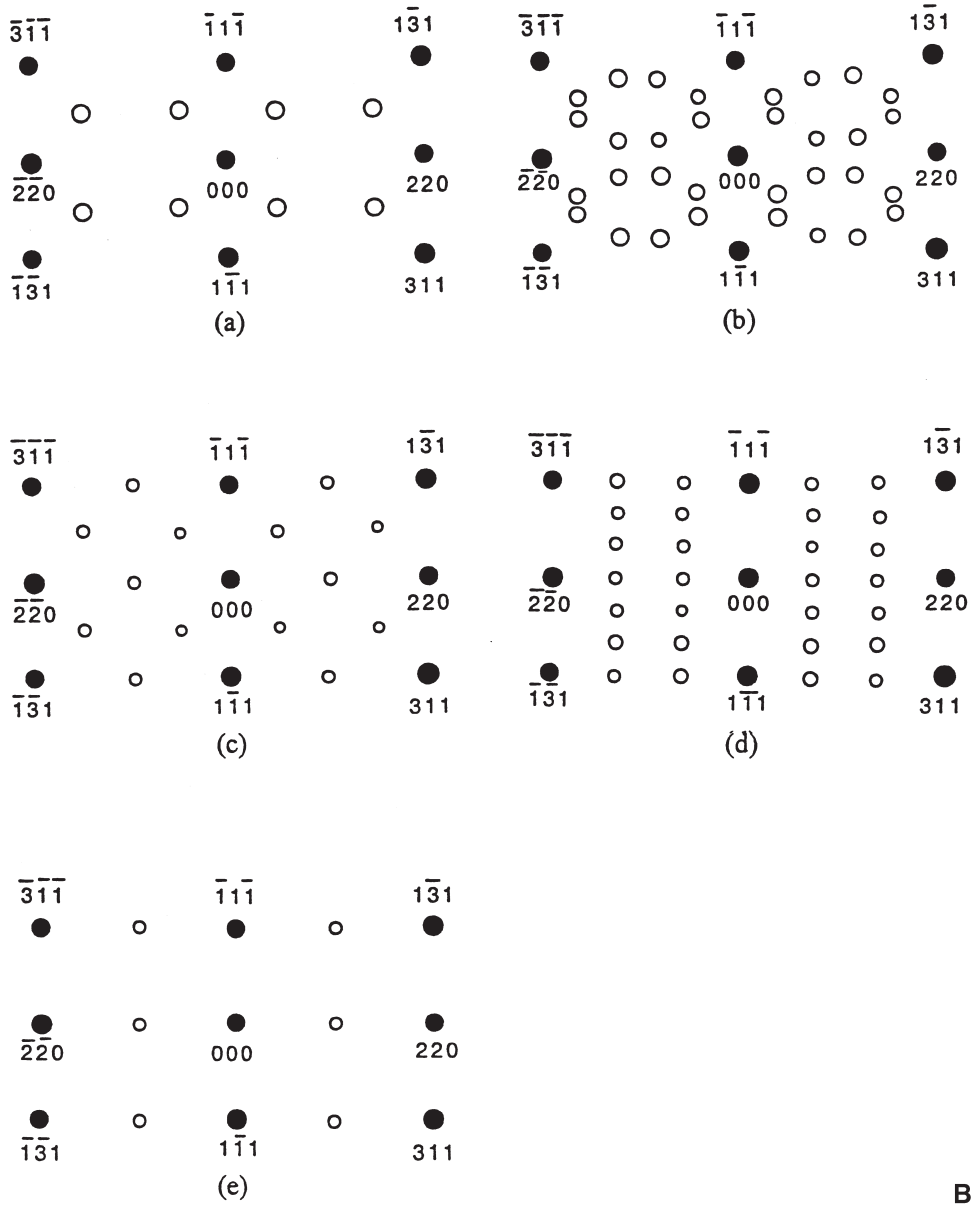

FIG. 6. Continued.

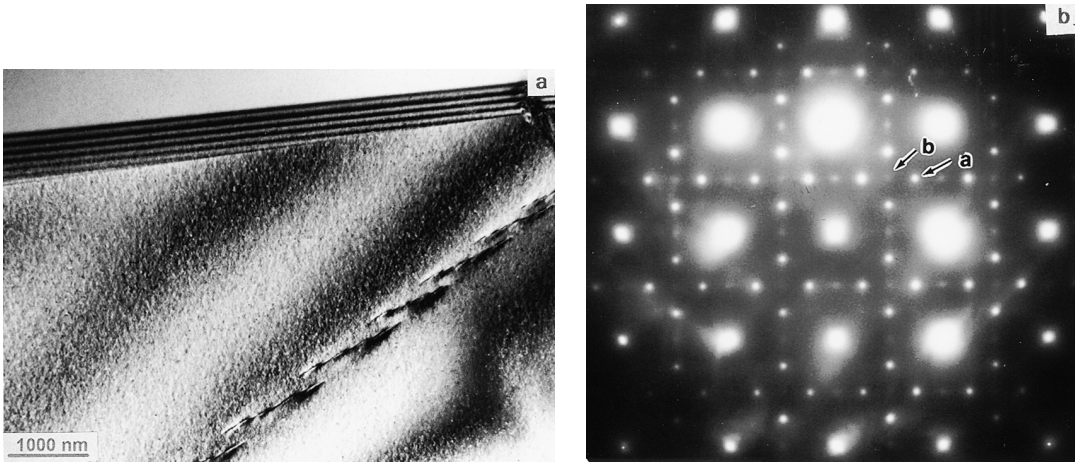

FIG. 7. (a) Microstructure and (001) diffraction pattern for solution heat-treated 2at.% Al alloy. (b) Diffraction spots from the SRO α (per arrow at "a") and the DO_{22} phase (per arrow at "b") are present.

and very small (e.g., 6–8Å) domains of the DO_{22} phase. However, no explanation for this structure in the quenched condition was offered.

The hardness of the 2 and 5at.% Al alloys is about the same as that of the binary alloy (Fig. 3), even though in the Al-containing alloys the structure contains fine domains of the metastable DO_{22} phase in the SRO α whereas the binary alloy is single phase SRO α. The marked hardness increase at 7 and 9at.% Al coincides with the appearance of the Ni_2Mo metastable phase in the form of fine domains, present along with fine domains of DO_{22}. Although for all of the Al-containing alloys the domain size is about the same, the complex microstructure of the mixed domain structure is apparently responsible for the high hardness.

CONCLUSIONS

It appears that Al additions to the base Ni_4Mo alloy enhance the decomposition of the short-range ordered α to metastable

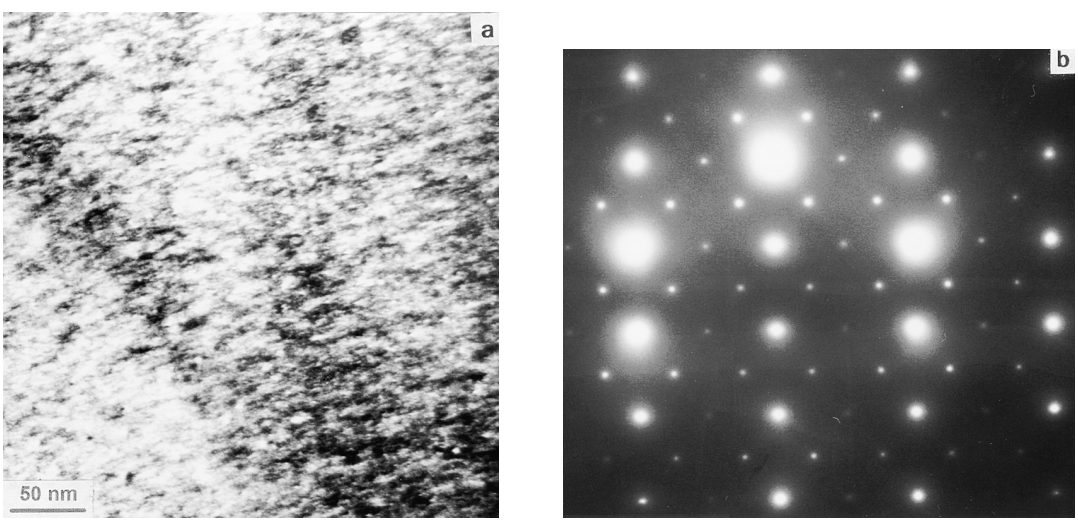

FIG. 8. Microstructure and (112) diffraction pattern for the solution heat-treated 5at.% Al alloy. Only the DO_{22} phase is present.

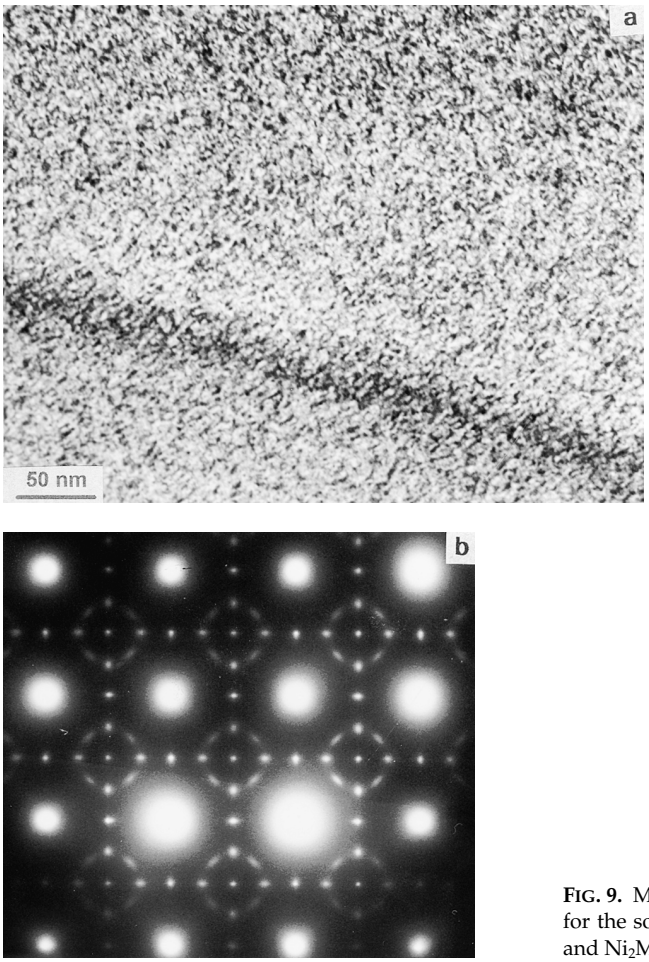

FIG. 9. Microstructure and (001) diffraction pattern for the solution heat-treated 7at.% Al alloy. The DO_{22} and Ni_2Mo phases are present.

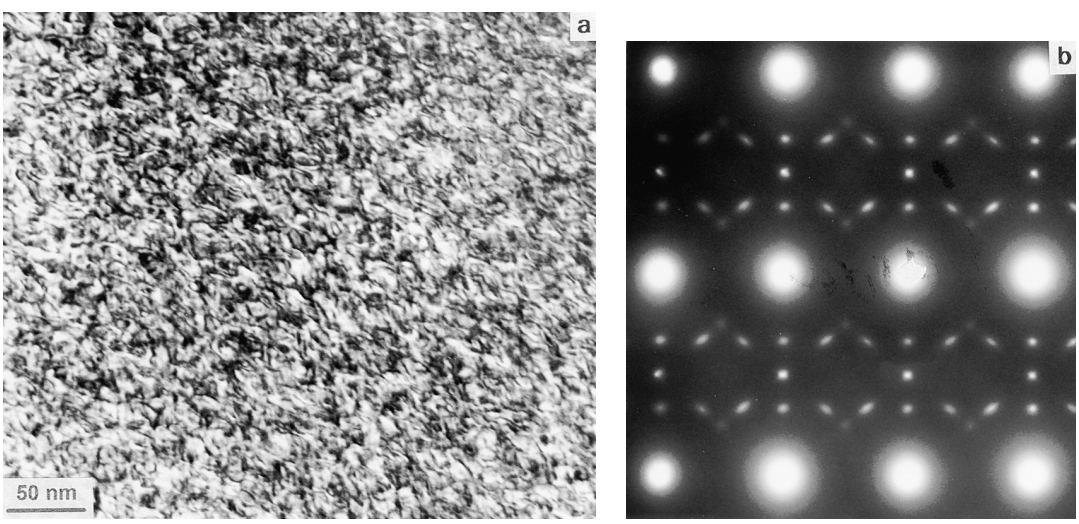

FIG. 10. Microstructure and (112) diffraction pattern for the solution heat treated 9at.% Al alloy. The structure consists of the DO_{22} and Mi_2Mo phases.

phases upon quenching from the solution heat treating temperature. The markedly higher hardness in this condition of the 7 and 9at.% Al is due to the presence of fine domains of the metastable Ni_2Mo phase, which are not present in the other alloys.

Some of this research was conducted at the Oak Ridge National Laboratory (ORNL) SHaRe User Facility, partially supported by the Division of Materials Sciences, U.S. Department of Energy under contracts DE-AC05-960R22464 with Lockheed Martin Energy Research Corporation and DE-AC05-760R00033 with Oak Ridge Associated Universities.

References

1. C. R. Brooks, J. E. Spruiell, and E. E. Stansbury: Physical metallurgy of nickel-molybdenum alloys. *International Metals Reviews* 29:210–248 (1984).
2. S. Cao, C. R. Brooks, and L. Allard: An *in situ* transmission electron microscopy study of ordering in a splat cooled Ni-20 at.% Mo alloy. *Microstructural Characterization* 34:87–95 (1995).
3. D. B. Miracle, K. A. Lark, V. Srinivasan, and H. A. Lipsitt: *Nickel-molybdenum*-aluminum phase equilibria, Metallurgical Transactions, 15A:481–486 (1984).
4. K. Vasudevan: Transmission electron microscopy study of phase transformations in ternary Ni_4Mo-based alloys containing 0 to 4 weight percent chromium, Ph. D. dissertation, The University of Tennessee, Knoxville, TN (1986).
5. P. L. Martin and J. C. Williams: Long range order in Ni_3Mo based ternary allows - I. Isothermal aging response, *Acta Metallurgica* 32:1681–1693 (1984).
6. G. Van Tendeloo: Short range order considerations and development of long range order in different Ni-Mo alloys. *Materials Science and Engineering* 26:209–220 (1976).
7. E. Ruedl, P. Delavignette, and S. Amelinckx: Electron diffraction and electron microscopic study of long- and short-range order in Ni_4Mo and of the substructure resulting from ordering. *physica status solidi* 28:305–328 (1968).
8. P. R. Okamoto and G. Thomas: On short range order and micro-domains in the Ni_4Mo system. *Acta Metallurgica* 19:825–841 (1971).
9. D. De Fontaine: k-Space symmetry rules for order-disorder reactions. *Acta Metallurgica* 23:553–571 (1975).
10. W. M. Stobbs and J.-P. A. A. Chevalier: The classification of short range order by electron microscopy. *Acta Metallurgica* 26:233–240 (1978).
11. J.-P. A. A. Chevalier and W. M. Stobbs: Short-range order and the disorder-order transformation in stoichiometric Ni_4Mo. *Acta Metallurgica* 27: 1197–1217 (1979).
12. J. Mayer and K. Urban: Spinodal ordering in Ni_4Mo. *Acta Metallurgical* 33:539–543 (1985).
13. M. Yamoto, T. Hashizume, and T. Sakurai: An atom-probe FIM study of the short-range order in an Ni_4Mo alloy. *Scripta Metallurgica* 19:357–360 (1985).
14. E. A. Kenik, T. A. Zagula, M. K. Miller, and J. Bentley: Ordering in Ni_4Mo by TEM and APFIM, in *Proceedings Forth-Fifth Annual Meeting, Electron Microscopy of America*, San Francisco Press, Inc., San Francisco, CA, pp. 214–215 (1987).
15. S. Banerjee, K. Urgan, and M. Wilkins: The transition from the short-range to the long-range ordered state in Ni_4Mo under electron radiation, in *Proc. Int. Conf. Solid-Solid Phase Transformations*, AIME, Warrendale, PA, pp. 311–315 (1982).
16. R. W. Carpenter and E. A. Kenik: In-situ radiation response of nickel-molybdenum alloys in an HVEM, in *High Voltage Electron Microscopy 1977*, T. Imura and H. Hashimoto, editors, Japanese Society of Electron Microscopy, Tokyo, Japan, pp. 577–580 (1977).
17. S. Banerjee, K. Urban, and M. Wilkins: Order-disorder transformation in Ni_4Mo under electron irradiation in a high-voltage electron microscope. *Acta Metallurgica* 32:299–311 (1984).
18. G. van Tendeloo, R. De Ridder, and S. Amelinckx: The DO_{22} intermediate phase in the Ni-Mo system. *physica status solidi (a)* 27:457–468 (1975).
19. G. Van Tendeloo: Short range order considerations and development of long range order in different Ni-Mo alloys. *Materials Science and Engineering* 26:209–220 (1976).
20. H. M. Tawancy: Formation of the DO_{22}-type superlattice during long-range ordering to Ni_4Mo in a Ni-Mo alloy. *Scripta Metallurgica* 18:343–346 (1984).
21. H. M. Tawancy and M. O. Aboelfotoh: Experimental observations of transient phases during long-range ordering to Ni_4Mo in a Ni-Mo-Fe-Cr alloy. *physica status solidi (a)* 99:461–466 (1987).
22. S. K. Das and G. Thomas: The metastable phase Ni_2Mo and the initial stages of ordering in Ni-Mo alloys. *physica status solidi (a)* 21:177–190 (1974).
23. T. Saburi, I. Komatsu, M. Yamamoto, S. Nenno, and Y. Mizutani: A new metastable phase Ni_2Mo. *Transactions Metallurgical Society AIME* 245:2348–2349 (1969).
24. V. Ya. Agaronik, A. M. Glezer, and N. G. Novoselova: Study of structural transformations in high-impedance nickel-molybdenum alloys with vanadium and aluminum. *Physics of Metals and Metallography* 44:104–112 (1978).

Received December 1997; accepted February 1999.